RESEARCH

# Preparation and characterization of activated carbons from Lemon Pulp for oxytetracycline removal

**Alper Solmaz · Mesut Karta · Tolga Depci ·
Talip Turna · Zeynel Abidin Sari**

**Abstract** This study aims to remove oxytetracycline (OTC) that harms the ecosystem, with activated carbon (LPAC) obtained from Lemon Pulp (LP). Characterization and properties of LPAC were analyzed by Brunauer–Emmett–Teller (BET), Fourier transform infrared spectroscopy (FTIR), scanning electron microscope (SEM), X-ray diffraction (XRD) and point of zero charge ($pH_{PZC}$) analyses. BET surface area, pore volume and $pH_{PZC}$ of LPAC produced by carbonization at 400 °C and activation with KOH at 800 °C were obtained as 1333.01 $m^2/g$, 0.391 $cm^3/g$, and 6.81, respectively. pH, reaction time, initial OTC concentration, and adsorbent amounts were optimized in the adsorption study performed with LPAC with high porosity and micropores. Kinetic evaluation was made with pseudo-first-order, pseudo-second-order, and intra-particle diffusion models and Freundlich, Langmuir, and Temkin equations are used to investigate their isotherms under reaction equilibrium conditions, and also the results were analyzed by statistical method (ANOVA). In pseudo-second-order kinetic and Freundlich isotherm models, where the best results were obtained, $R^2$ values were calculated as 0.999 and 0.995, respectively. Maximum OTC removal efficiency was found as 104.22 mg/g. Overall, this research indicates that LPAC for the treatment of water contaminated with antibiotics is environmentally friendly green material.

**Keywords** Activated carbon · Adsorption · Lemon Pulp · Oxytetracycline

A. Solmaz (✉)
Department of Environmental Protection
and Control-Iskenderun Vocational School of Higher
Education, Iskenderun Technical University, Hatay, Turkey
e-mail: alper.solmaz@iste.edu.tr

M. Karta · Z. A. Sari
Department of Metallurgy-Iskenderun Vocational School
of Higher Education, Iskenderun Technical University,
Hatay, Turkey

T. Depci
Department of Petroleum and Natural Gas Engineering,
Iskenderun Technical University, Hatay, Turkey

T. Turna
Department of Parks and Garden Plants-Diyarbakır
Vocational School of Higher Education, Dicle University,
Diyarbakır, Turkey

## Introduction

According to the amount of antibiotic use in 76 countries, it is estimated that the defined daily dose (DDD) increased from 21.1 million DDDs in 2000 to 34.8 million DDDs in 2015 with an increase of 65%, and it will reach 42 billion DDDs in 2030 (Klein et al., 2018). On the other hand, in a study conducted on 41 countries in 2017, it is estimated that the amount of antibiotics used in animal husbandry is approximately 93,309 tons, and this value will increase to 104,079 tons in 2030 (Tiseo et al., 2020). Depending on the

chemical properties and metabolized status of these antibiotics used, they can be excreted in the feces or urine at a rate of 5–90%. This excretion can be as the basic compound or in the bound metabolites (Avisar et al., 2009; Daghrir & Drogui, 2013). These antibiotic residues, which are excreted directly or indirectly from hospitals (waste and wastewater), animal breeding facilities, industrial facilities, aquaculture fields, and human feces or urine, reach wastewater treatment plants (Kümmerer et al., 2000; Li et al., 2021). Since almost all general wastewater treatment plants in the world are designed on the basis of removing C, N, P, and some other main pollutants, it has been proven by many studies that these existing wastewater treatment plants are not sufficient for the removal of antibiotics (Afshin et al., 2020; Ahmadfazeli et al., 2021; Al-Gheethi et al., 2015; Lien et al., 2016; Russell & Yost, 2021).

It is inevitable that these antibiotics leaving the wastewater treatment plants reach the receiving environments and enter the ecosystem (Karthikeyan & Meyer, 2006; Shokoohi et al., 2018a). Nearly 40 years have passed since the first detection of the presence of antibiotics called tetracycline and erythromycin in river water near a fish farm in the receiving environment (Watts et al., 1984). During this time, sulfonamides, fluoroquinolone, macrolide trimethoprim, and many other types of antibiotic residues were found in groundwater (F. Huang et al., 2020; Shokoohi et al., 2018b; Zainab et al., 2020), such as river lake, etc. in surface waters (Balzer et al., 2016; Sta Ana et al., 2021; Yang et al., 2018), at the influent and effluent of treatment plants (Karthikeyan & Meyer, 2006; Langbehn et al., 2021), in soil and coastal waters (Yang et al., 2018), in garbage leachate from landfills (G. Chen et al., 2021), in fish farm wastewater (Liu et al., 2017), and in livestock farm wastewater (Gaballah et al., 2021; Muhammad et al., 2020); dozens of studies have been conducted on the detection of antibiotics.

Physical, chemical, and biological removal studies of these antibiotics are carried out by methods such as coagulation-flocculation systems, membrane separation techniques, adsorption, biological degradation, artificial wetlands, advanced oxidation processes, and combined treatment systems. Since these and many similar studies have low removal rates and high operating costs, it is very difficult to apply these studies on a large scale (A. Huang et al., 2021; Wang & Zhuan, 2020). Except for the adsorption processes carried out with AC, almost all the above-mentioned methods may result in incomplete removal of antibiotics (especially on an industrial scale) and the emergence of more dangerous by-products than the first compound (Adams et al., 2002; Lach et al., 2021; Westerhoff et al., 2005).

Removal of pharmaceuticals from wastewater using AC has attracted great interest in recent years (Beltrame et al., 2018; Braghiroli et al., 2018). However, in terms of being economical and most importantly sustainable, researches on the production of high-quality and low-cost AC have gained momentum today. For this, the production of AC from wastes and biomass-based materials (banana, rice, tea waste, wood, walnut shell, etc.) is very popular as an ecofriendly process (Kumar Jha et al., 2021). Thanks to this green and sustainable system, wastes gain economic importance, and the high value-added product is used to eliminate a waste (Adeleye et al., 2021).

The use of agricultural wastes as adsorbent is of great interest due to their abundance, low cost, high fixed carbon content, and porous structure (Bhatnagar et al., 2009; Rashtbari et al., 2022). In addition, fruit peels consist of valuable amounts of lignin, cellulose, hemicellulose, carboxyl, hydroxyl, pectin substances, and amide surface functional groups. This generally increases the adsorbent-adsorbate interactions. If LP is taken into account here, they contain higher amounts of polysaccharides such as pectin (33.87%) and cellulose (14.35%) compared to citrus peels, which are similar agricultural products. These polysaccharides are rich in functional groups such as carboxylic (in galacturonic acids) and hydroxyl (in cellulose). Therefore, factors such as the richness of functional groups, good physical stability, low cost, and easy availability in the climatic region are effective factors in the selection of LP in our study (Ramutshatsha-Makhwedzha et al., 2022; Singh and Shukla n.d.; Thirumavalavan et al., 2011). Useless waste generated after the valuable liquid in citrus fruits is extracted can be obtained free of charge from these enterprises. The pulp remaining after lemon juice extraction can be used as a cheap adsorbent because it is cheap and abundant (Okon Eddy et al., 2022; Ramutshatsha-Makhwedzha et al., 2022). These carbon-rich wastes cause negative environmental effects when landfilled, as they can form leachate that can lead to greenhouse gas emissions. Thanks to

the evaluation of these wastes, the danger posed by them in terms of the environment is prevented. For these reasons, waste minimization will be realized and economic benefit will be achieved thanks to the production of AC from LP, and thus an alternative product to commercial ACs will emerge.

In this study, AC was obtained from LP the framework of green chemistry. The textural characteristics BET, SEM, FTIR, XRD, and $pH_{PZC}$ of the obtained AC were determined. Adsorption isotherm and kinetics were determined by removing OTC with the produced AC and statistical analysis (ANOVA) of the obtained results was made.

## Material and method

### Chemicals

All the chemicals we used in our experiment were of analytical purity, and the solutions were prepared with distilled water. OTC is originated from Merck (Germany) and its molecular formula is $C_{22}H_{24}N_2O_9$ and its molecular weight is 460.33 g/mol. KOH, NaCl, NaOH, and $H_2SO_4$ were purchased from Merck (Germany). Also, Ar gases (pure 99.99%) were purchased from local laboratories (Linde Gas, Turkey). In addition, 0.01 M NaOH and 0.01 M $H_2SO_4$ were used to balance the pH of the solutions in experimental studies.

### Synthesis of LPAC

LP were obtained from Juice Factory, Mersin, Turkey and dried at 105 °C for 24 h. The dried sample thereafter in a tube furnace (MSE Furnace) continued to be heated at a rate of 10 °C min$^{-1}$ to 400 °C under Ar atmosphere for carbonization. This process continued for 1 h. Subsequently, carbonized sample for activation mixed with KOH, in mass ratio of 1/3. By using KOH as the activator instead of activators such as $ZnCl_2$ and $H_3PO_4$, metallic K ions are mixed into the carbon network and accelerate the carbon loss, thus enabling the expansion of the pores, and it provides the formation of -OH functional groups. Thus, the use of KOH results in a larger specific surface area as well as better pore development (Hui & Zaini, 2015; Joseph et al., 2006). In addition, KOH is generally preferred because it is less harmful to the environment

than other chemical activating agents (Mamaní et al., 2019). Then LPAC obtained 10 °C min$^{-1}$ to 800 °C under Ar atmosphere and maintained at this temperature for 1 h. The obtained LPAC material was washed with 0.5 M HCl solution during filtration to remove inorganic ions. It was then washed with distilled water until it reached neutral (about 7.00) with distilled water and then left to dry in an oven at 100 °C for approximately one night. Finally, it was stored in desiccator for further experiments. Since nitrogen gas is not inert, its structure changes at high temperatures and a nitride structure is formed. If this happens, a hard layer may form on the surface of the product. In order to avoid this, the use of Ar gas was preferred in the environment.

### Determination of the point of zero charge ($pH_{PZC}$)

The point of zero charge ($pH_{PZC}$) at which the activation of the acidic/basic functional groups of LPAC is constant is determined. For this, 0.01 M NaCl solution was prepared for 5 Erlenmeyer flasks of 50 mL, 0.1 g of LPAC was added into it. The initial pH of the solutions was adjusted between 3.0 and 11.0. 0.1 M $H_2SO_4$, and 0.1 M NaOH were used to accomplish this. All of solutions stirred at room temperature for 48 h. The cutoff point obtained from the graph was determined as $pH_{PZC}$ by reading the final pH's (Farahani et al., 2011; Peyghami et al., 2021; Rashtbari et al., 2020).

### Adsorption studies

Batch studies were carried out in 50 mL flasks. Optimum pH was determined by first treating the flasks with 0.02 gr LPAC added at 25 mg/L OTC concentration at 60 rpm at varying pH (2.0–8.0). Then, variable LPAC amounts (0.005–0.08 g) and stirring speeds (60–240 rpm) at optimum pH were determined, respectively, and finally, optimum conditions were determined for initial dosages in the range of 10–150 mg/L. In the experiments, OTC concentrations were measured at a wavelength of 354 nm in a UV–Vis spectrophotometer (Peak E-1000UV) after the upper phase water was passed through a 0.45-membrane filter (Aghababaei et al., 2017; Berger et al., 2019; Lach et al., 2021; Nayeri et al., 2019; Sun et al., 2013). Experimental analysis

was carried out in three repetitions, and the produced LPAC was used once.

The removal efficiency (R) was made according to Eq. 1.

$$R(\%) = \frac{C_0 - C_e}{C_0} \times 100 \tag{1}$$

where $C_0$ and $C_e$ are the initial and equilibrium concentration (mg/L) of OTC, respectively.

OTC amount in equilibrium is calculated by Eq. 2.

$$q_e = \frac{(C_0 - C_{e)} \times V}{m} \tag{2}$$

where $C_0$ and $C_e$ are the initial and equilibrium concentration (mg/L) of OTC, respectively; $m$ adsorbent amount (g) and $V$ is the total volume of solution (L).

Adsorption kinetics

The pseudo-first-order reaction equation, first proposed by Lagergren, is as in Eq. 3 (Wang & Guo, 2020a):

$$\frac{dq_t}{d_t} = K_1(q_{e-}q_t) \tag{3}$$

Equation 4 is obtained if the equation is linearized:

$$Log(q_e - q_t) = Log q_{e-} \frac{K_1}{2.303} t \tag{4}$$

Here, $q_e$ and $q_t$ denote the amount of OTC (mg/L) at any time $t$ in equilibrium, respectively, and the $K_1$ pseudo-first-order reaction constant (1/min).

Again, the pseudo-second-order reaction equation, first proposed by Ho et al., is as in Eq. 6 (Ho et al., 1996):

$$\frac{dq_t}{d_t} = K_2(q_{e-}q_t)^2 \tag{6}$$

Equation 7 is obtained if the equation is linearized:

$$\frac{t}{q_t} = \frac{1}{K_2 q_e^2} + \frac{1}{q_e} t \tag{7}$$

Here, $q_e$ and $q_t$ denote the amount of OTC (mg/g) at any time $t$ in equilibrium, respectively, and the $K_2$ pseudo-second-order reaction constant (1/min).

Again, the Intra-particle diffusion model equation proposed by Masinga et al. is presented in Eq. 8 (Masinga et al., 2022);

$$q_t = K_{id} t^{1/2} + C \tag{8}$$

Here again, $q_t$ denotes the amount of OTC (mg/g) at a time $t$, $C$ the OTC concentration removed (mg/L), and the $K_{id}$ intra-particle diffusion model constant. $K_{id}$ is obtained by plotting the value of $t^{1/2}$ against the value of $q_t$ in the equation.

Adsorption isotherms

The equations listed below were used to determine the adsorption isotherms of the experimental studies;

The Freundlich equation is presented in Eq. 9, and its linearized form is presented in Eq. 10 (Wang & Guo, 2020a);

$$q_e = K_F C_e^{1/n} \tag{9}$$

$$ln q_e = ln K_F + \frac{1}{n} ln C_e \tag{10}$$

where $q_e$ is the amount of OTC adsorbed at equilibrium (mg/g); $C_e$ is the concentration of OTC at equilibrium (mg/L); and $K_F$ and $n$ represent Freundlich constants. If the equation is linearized, the following equation is reached:

The Langmuir equation is presented in Eq. 11, and its linearized form is presented in Eq. 12 (Wang & Guo, 2020a);

$$q_e = \frac{Q_0 K_1 C_e}{1 + K_1 C_e} \tag{11}$$

$$\frac{C_e}{q_e} = \frac{1}{K_L} + \frac{a_L}{K_L} C_e \tag{12}$$

In order to determine the suitability of the adsorption process in this isotherm, the "Dispersion Constant $R_L$" must be determined. Equation 13 is used for this.

$$R_L = \frac{1}{1 + a_L C_0} \tag{13}$$

Here again, $C_e$ is the equilibrium concentration of OTC (mg/L); $q_e$ is indicates the amount of OTC adsorbed at equilibrium; $K_0$ is indicates the maximum

adsorption amount (mg/g); $K_L$ is Langmuir adsorption constant (L/mg); $a_L$ is Langmuir constant (L/mg).

The Temkin equation is presented in Eq. 14, and its linearized form is presented in Eq. 15 (Temkin, 1940);

$$q_e = Bln(A_T C_e) \tag{14}$$

$$q_e = BlnA_T + BlnC_e \tag{15}$$

Here again, $q_e$ is the amount of OTC adsorbed at equilibrium, $B$ is the cautious constant (J/mol), which is expressed as $B = \frac{RT}{b_T}$. Here, $R$ represents the universal gas constant (8.314 j/mol.K), T temperature (K), $b_T$ is the heat of adsorption isotherm constant (kj/mol), and $C_e$ is the equilibrium concentration of OTC (mg/L).

## Statistical analysis

Minitab statistical software was used to perform statistical analysis of the results obtained in the experimental studies. Here, a statistical evaluation was made only on the change in the amount of adsorbent. The results of the statistical evaluation were verified by comparing analysis of variance (ANOVA) and correlation coefficient ($R^2$). $p$ values, one of the most important findings in the statistical evaluation, were used to emphasize the importance of the amount of pollutant/adsorbent (10–150 mg/L) on the target outputs (95% confidence level). It is known that when the $p$ values are less than or equal to 0.05, the amount of adsorbent represents an important amount, and when it is large, it represents an insignificant amount. Also, regression analysis was performed on the amount of adsorbent.

## **Results**

### Characteristic of LPAC

### *Chemical analysis*

Chemical analyses of the raw LP were carried out by ICP-OES (inductively coupled plasma optical emission spectrometer, Perkin-Elmer, Optima 2000DV) in clear supernatant that was obtained by the microwave digestion process. The results of

**Table 1** Chemical characteristics of raw LP

| Element | C | H | N | S | O |
|---------|-------|------|------|-------|-------|
| % | 45.32 | 6.74 | 1.95 | 0.379 | 45.62 |

**Table 2** Surface area and pore size distribution of the LPAC sample prepared at 800 °C

| Surface area (m²/g) | | Pore volume (cm³/g) | | Mean pore size (nm) |
|---------|---------|---------|---------|---------|
| $A_{BET}$ | $A_{micro}$ | $V_{total}$ | $V_{micro}$ | D |
| 1333.01 | 820.20 | 0.684 | 0.394 | 2.055 |

the full chemical analyses are shown in Table. 1. In addition, the ash analysis value of the raw sample made in the muffle furnace was determined as 2.42%.

### *Textural characteristics of adsorbents*

BET (TriStar II Plus 3.02) was used to determine the specific surface area (BET) of the adsorbents, their pore size, their distribution and also the pore volume, and the obtained values are presented in Table 2. In addition, the nitrogen adsorption/desorption isotherm of LPAC carbonized at 800 °C is presented in Fig. 1. When Fig. 1 is examined, it is clear that there is a rapid increase at low relative pressures compared to the adsorption–desorption isotherm. Moreover, it can be seen that the slope decreases as the relative pressure increases. When the obtained figure is compared with the classification made by the International Union of Fundamental and Applied Chemistry (IUPAC), it is seen that this is a type 1 isotherm (Naeem et al., 2017). Therefore, the fact that the LPAC we produce at 800 °C has a micropore structure is also confirmed by the type I isotherm. If the pore volume and diameter of our adsorbent are evaluated, it was determined as 0.285 cm³/g and 2.336 nm, respectively, according to the results of BET analysis. According to the classification made by IUPAC in the literature, pore diameters are divided into 3, these are micro pore (< 2 nm), meso pore (2–50 nm), and macro pore (> 50 nm), respectively (Zdravkov et al., 2007).
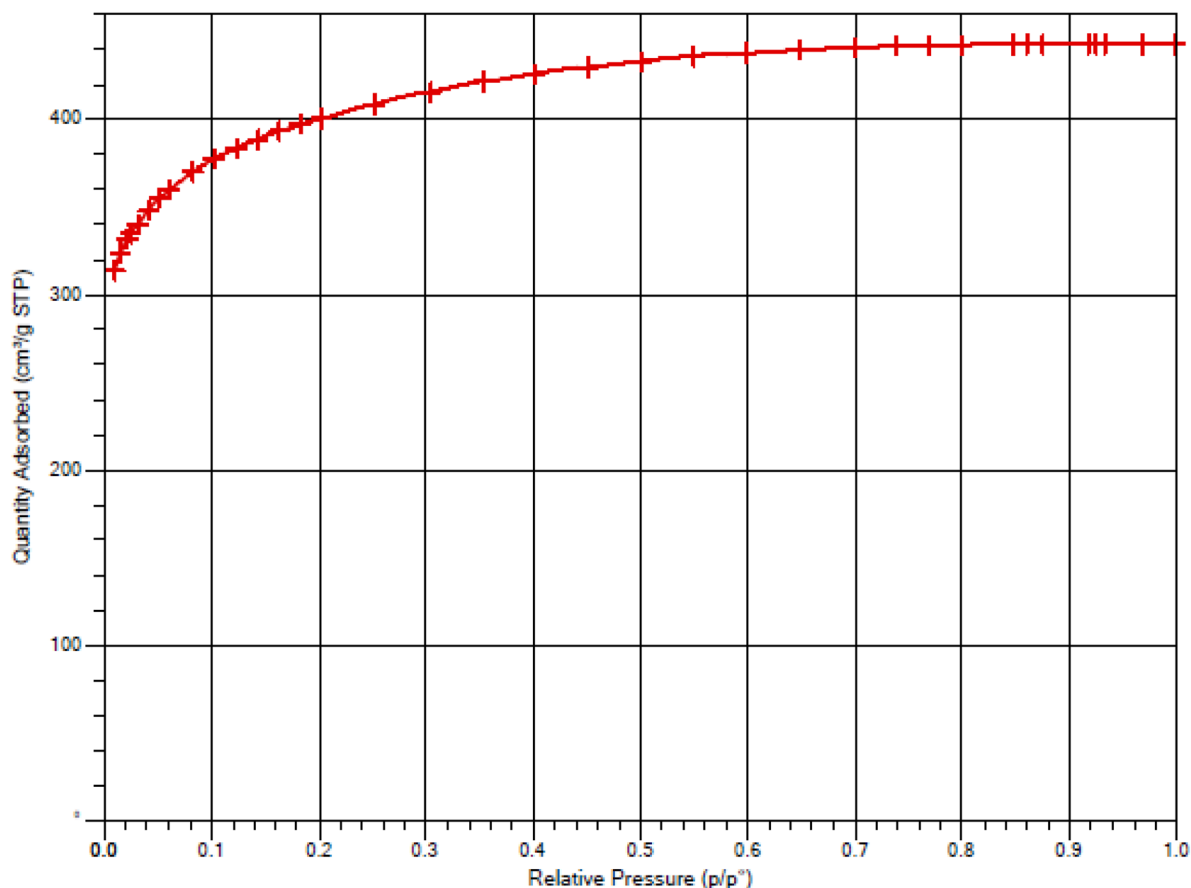
**Fig. 1** Nitrogen adsorption–desorption isotherm of 800 °C LPAC

*Scanning electron microscopy (SEM)*

SEM (Thermo Fisher Scientific Apreo S) images of modified and after adsorption of OTC carbon are shown in Fig. 2. The micrograph presented in Fig. 2A is the porous structure of LPAC before adsorption. In Fig. 2A, there are easily many pores and pores of variable diameter on the surface of the LPAC. These pores show that OTC molecules have a large surface area and space for interaction and attachment. On the other hand, the SEM image after OTC adsorption is presented in Fig. 2B. As can be seen in Fig. 2B according to the micrograph taken after OTC adsorption, the pores on the surface of the LPAC started to fill and close. Therefore, it showed a very serious variation after the adsorption process. This is a clear indication that OTC is adsorbed into the pores and voids on the LPAC.

*Surface functional groups on the adsorbents*

According to the figure, surfactant groups such as $C=O$ and $C=C$ were observed here. In addition, the OH group is located at 3369 and 3359 cm$^{-1}$. The peak observed at 675 cm$^{-1}$ in the figure represents the C–H interaction on the surface of the LPAC. In addition, large regions observed around 1102–1062 cm$^{-1}$ may be related to anhydrides (Foo & Hameed, 2012), alcoholic or carboxylic or possibly phenolic groups' stretching vibration (C–O), but it is somewhat difficult to distinguish because their peaks overlap. The 1539 cm$^{-1}$ point can be expressed as the stretching vibration of $NO_2$. On the other hand, the peaks seen around 1561–1540 cm$^{-1}$ correspond to the stretching vibration of the aromatic $C=C$ skeletal structure and are also thought to be related to sp2-linked carbon allotropes. The peak seen at 2087 cm$^{-1}$ can be
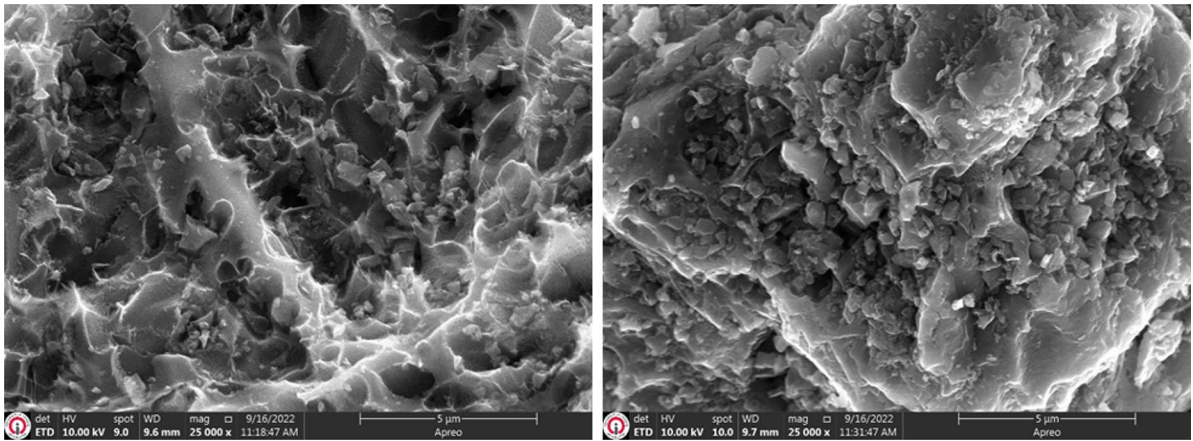
**Fig. 2** SEM (25,000×) images of LPAC before adsorption (**A**) and LPAC after adsorption of OTC (**B**)

expressed as carbonate group vibration. In the band observed at 2777 cm$^{-1}$, it can be stated that the isocyanate group corresponds to the vibration of –NCO. In addition, the peak observed at 2650 cm$^{-1}$ was caused by –CH stretching (Fig. 3).

*X-ray diffraction analysis (XRD)*

The crystal structure of LPAC was analyzed by XRD (Rigaku, Miniflex 600) and presented in Fig. 4. Some small peaks seen in the figure are due to residual mineral after activation with potassium hydroxide during production (Al-Qodah & Shawabkah, 2009). In addition, the peak expansion may depend on the crystallite size as well as on the stresses and diffraction properties. On the other hand, there may be changes in the average crystalline peak shift depending on the effect of the chemical used as the activating agent and the components of the LP, which is our raw material. Here, silica and ash content were removed by the

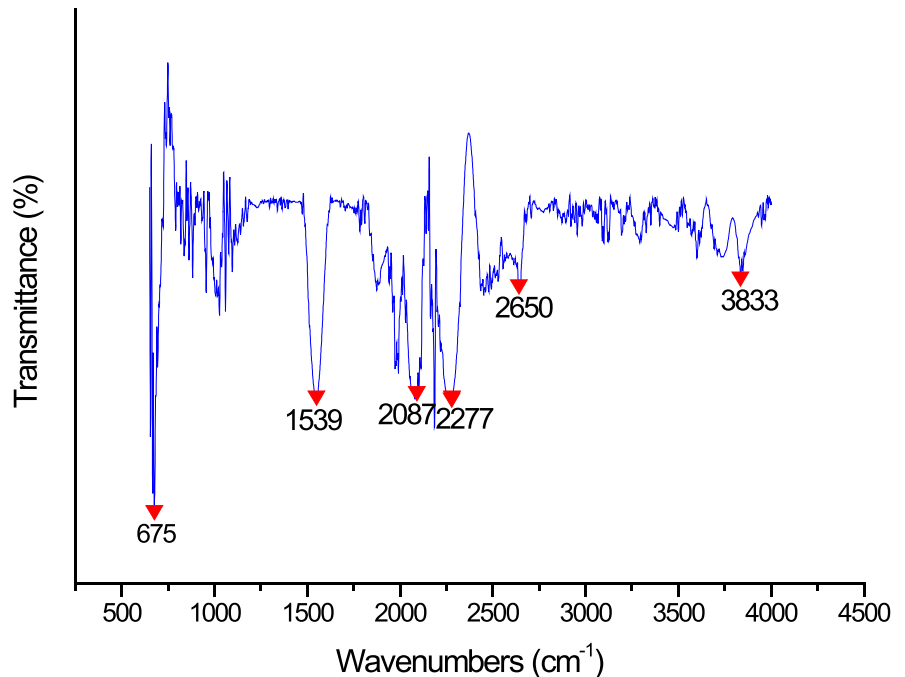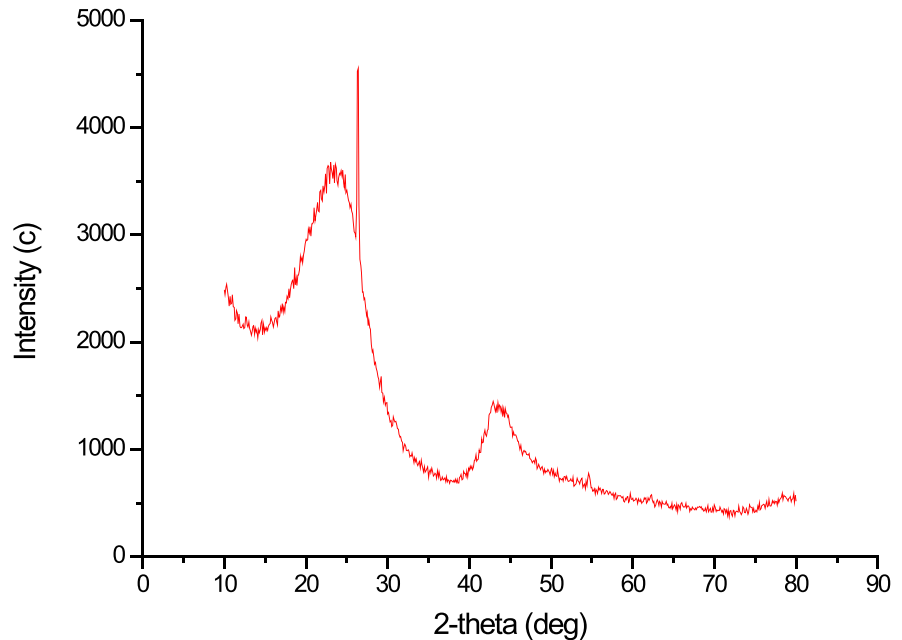**Fig. 3** FTIR spectra of the LPAC (before adsorption)

**Fig.4** The X-ray diffraction pattern of LPAC (before adsorption)



KOH activating agent. A slight variation in the XRD pattern of LPAC was observed due to the activating agent used.

*Point of zero charge (pH_PZC)*

The $pH_{PZC}$ of an adsorbent is the point at which the net electrical charge on its surface is zero. If the adsorption takes place above the current $pH_{PZC}$ value, the adsorbent surface becomes a negative charge due to the decrease in the proton concentration, that is, the situation is anionic. However, if the sorption takes place below the current $pH_{PZC}$ value, extra protons are added to the acidic functional groups on the adsorbent surface, and these functional groups can be defined as cationic since these functional groups remain neutral (Hashem et al., 2021). The test results for determining the zero-charge point of the produced LPAC are presented in Fig. 5. The $pH_{PZC}$ of the obtained activated carbon was measured as 6.81.

Adsorptive removal of OTC

*Effect of pH*

pH is a key parameter due to the nature of the functional groups of the substance used as the adsorbent and the degree of ionization of the substance

to be removed in the solution (Abdollahzadeh et al., 2020). OTC generally changes to cationic ($OTC^+$) and uncharged ($OTC^0$) form in the pH range of 3.30–7.30, as the pH increases, $OTC^-$ and $OTC^{-2}$ form the molecule. Therefore, as a result of pH increase, the negative form in the solution will be excessive, which will cause electrostatic repulsion, and as a natural result, the adsorption capacity will decrease (Aghababaei et al., 2017; Ötker & Akmehmet-Balcioğlu, 2005). Figure 6 shows the removal efficiencies of OTC at varying pH in the presence of 0.2 g adsorbent. In a study on UV–VIS spectrophotometer measurement of OTC, it was observed that OTC peaks at wavelengths between 354 and 366 nm in the range of pH 3.68 and pH 8.57, and in our study, the maximum peak was measured at 354 nm (Berger et al., 2019). In the OTC removal study performed with AC obtained from cotton linter fibers, it was noted that there was a decrease of pH around 5.00 to 6.00 (Berger et al., 2019; Sun et al., 2012). On the other hand, while the adsorption capacity reached the maximum at OTC concentration pH 5.00 by modifying the commercial AC, it was observed that the adsorption capacity decreased with the increase in pH (Lach et al., 2021). In our study, the amount of OTC adsorbed by LPAC was calculated as 91.18% at pH 5.00, while this value was measured as 62.55% at pH 8.00.

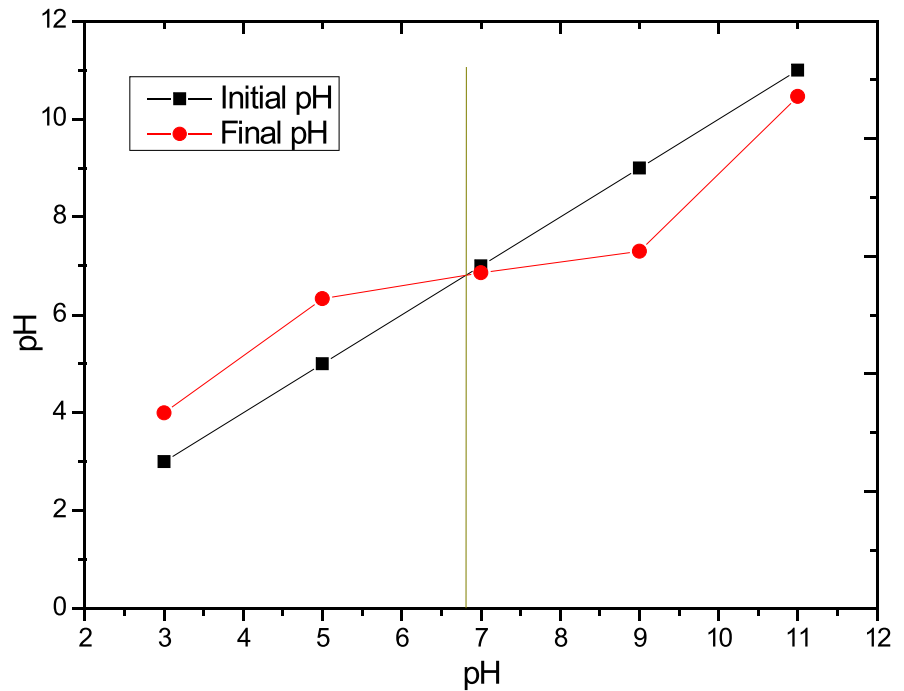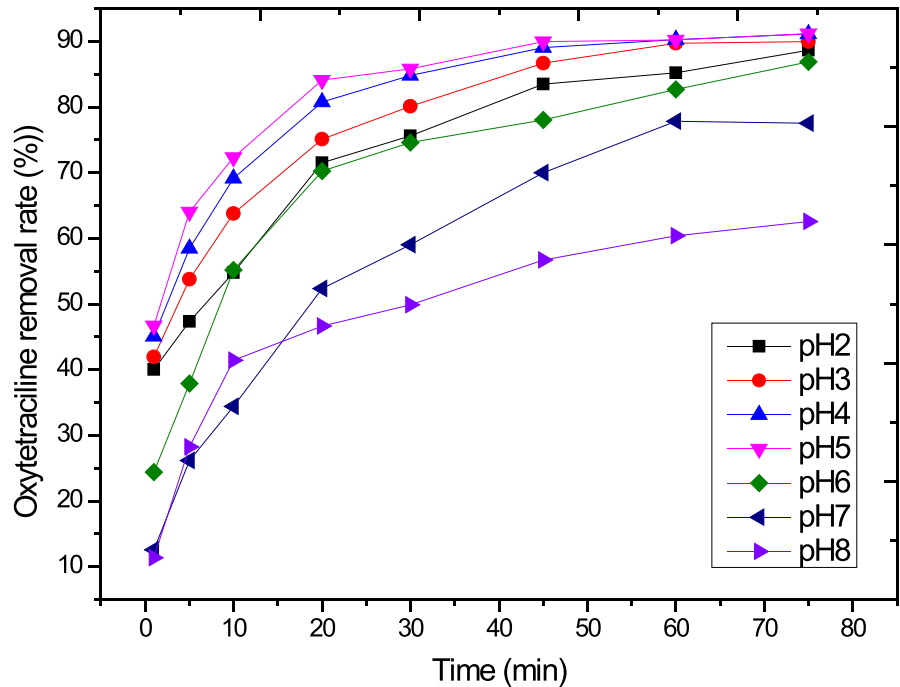**Fig. 5** Point zero charge of LPAC made from LP (T: 25 °C)



**Fig. 6** Removal efficiencies of OTC at varying pHs over time (T: 25 °C, adsorbent: 0.2 g)



*Adsorption kinetics*

In adsorption, the rate of uptake of the solute by the adsorbent is determined. This event is possible by knowing the time required for the reaction to occur. First of all, in Fig. 7, the adsorbent kinetics of OTC over time at different initial concentrations in the presence of 0.2 g adsorbent at 25 °C, pH: 5.0 is seen.
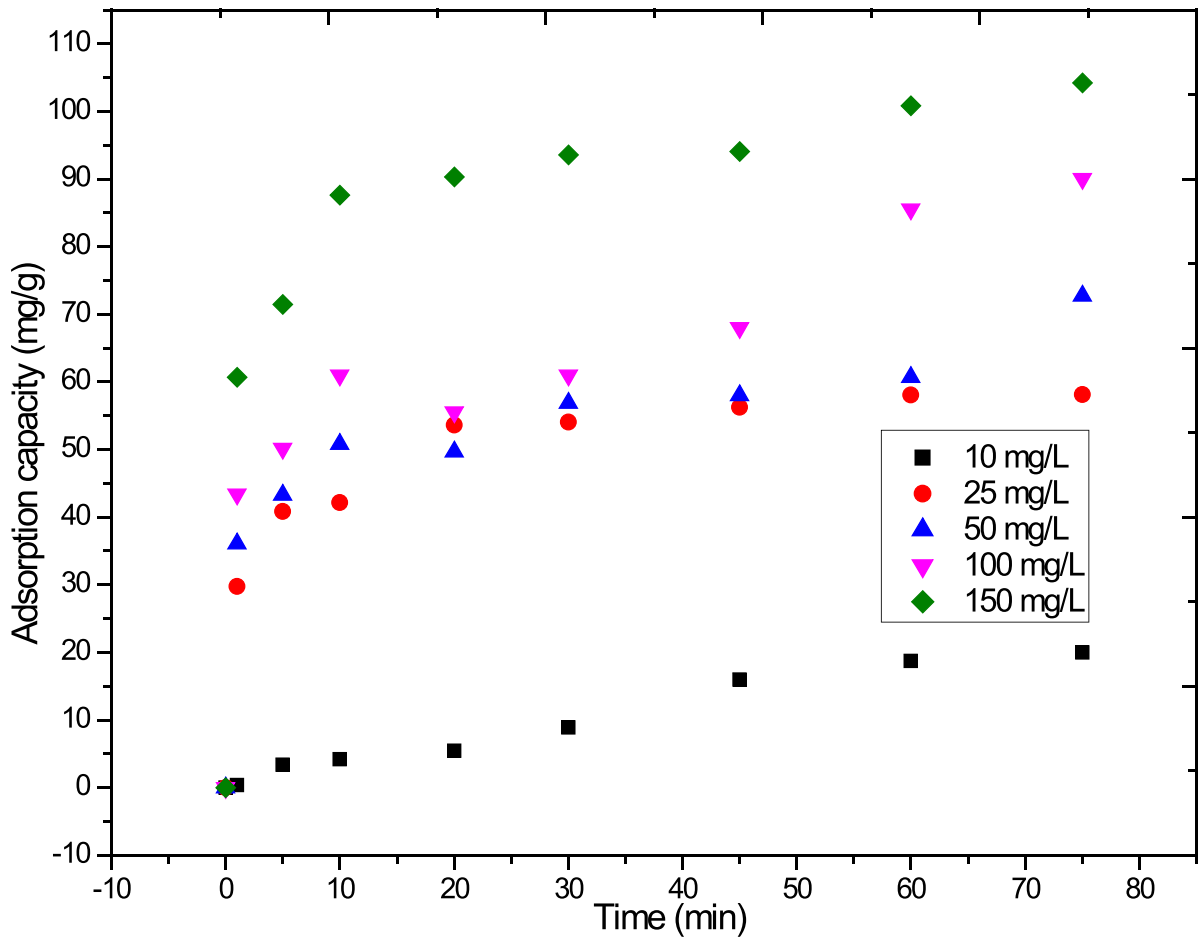
**Fig. 7** Adsorption rates versus time at different initial concentrations (T: 25 °C, pH: 5.0, and adsorbent: 0.2 g)

According to the Fig. 7, it can be said that the adsorption is quite fast in the initial times, and its speed slows down as the time progresses. In the first 20 min, the adsorption rate was calculated as 21.89, 84.09, 39.76, 22.4%, and 24.10% at the initial concentrations of 10, 25, 50, 100, and 150 mg/L, respectively.

In addition, the performance of an adsorbent is evaluated by adsorption kinetics. In other words, in order to complete the reaction in the kinetic analysis, it is possible for the solute in the solution (which can be expressed as a pollutant for us) to be adsorbed by the adsorbent (AC) in 4 stages, in order of macro convection, micro transport, intra-particle diffusion, and sorption. In addition, if the adsorbent is in a stationary phase, the rate determining step is the

1st step, and if the speed is increased here, the surface layer thickness decreases, and the adsorption rate increases. The second step can be defined as the first times (minutes) of adsorption in general. Since the speed is too fast to be defined in the 4th step, the 2nd and 3rd steps can clearly define the rate of adsorption (Qiu et al., 2009; Wang & Guo, 2020b). In our study, pseudo-first-order, pseudo-second-order, and intra-particle diffusion models, which are widely used in environmental applications, were studied, and the kinetic parameters obtained from these models are presented in Table 3. According to Table 3, it was determined that the adsorption of OTC on LPAC was more suitable for the pseudo-second-order model since it had a high $R^2$ (0.999) value. Therefore, it can

**Table 3** Calculated kinetic parameters of OTC sorption onto LPAC

| Kinetic equation constants | Constants and error functions | 25 °C |
|---|---|---|
| Pseudo-first-order | $q_{max}$ (mg/g) | 104.22 |
| | $k_1$($h^{-1}$) | −0.089 |
| | $R^2$ | 0.904 |
| Pseudo-second-order | $q_{max}$ (mg/g) | 23.42 |
| | $k_1$($h^{-1}$) | 0.017 |
| | $R^2$ | 0.999 |
| Intra-particle diffusion model | $K_{id}$ (mg/g.$h^{0.5}$) | 0.244 |
| | $R^2$ | 0.870 |

be said that this process is a chemical sorption, and therefore there is a strong electrostatic attraction force or ion exchange on the surface of the adsorbent (Kan et al., 2017; Sun et al., 2012).

*Adsorption isotherms*

The mathematical expressions of the adsorption isotherms can be defined as the graphical representation of the adsorbent with the pollutant remaining in solution at equilibrium. It is known that there are more than 200 mathematical models, and by modeling these isotherm data, the adsorbent capacities are determined, while system designs and performance are realized (X. Chen & Yao, 2015; Wang & Guo, 2020a). Langmuir, Freundlich, and Temkin isotherms are generally preferred in environmental applications (Mozaffari Majd et al., 2022; Rajahmundry et al., 2021). The Langmuir isotherm is defined for gas–solid phase adsorption and measures the adsorbing capacity of adsorbents. In this isotherm, the open surface fraction of the adsorbent is proportional to the adsorption equilibrium. Desorption is proportional to the fraction of the coated adsorbent surface. In this isotherm, it is assumed that it takes place in a monolayer region, and there is no interaction between adsorbed molecules (Ayawei et al., 2017; Langmuir, 1916). Freundlich isotherm, on the other hand, refers to adsorption theoretically on heterogeneous surfaces; the attraction is not homogeneous and therefore a non-ideal sorption (Freundlich, 1906; Mozaffari Majd et al., 2022). In the Temkin isotherm, however, its takes into

account the interactions of the adsorbates among themselves and claims that this interaction will decrease linearly, not logarithmically (Rajahmundry et al., 2021; Temkin, 1940).

The adsorption isotherms of OTC are presented in Fig. 8. The figure represents the Langmuir (A), Freundlich (B), and Temkin (C) isotherms, respectively.

In addition, the correlation coefficients obtained from the models are presented in Table 4. The highest $R^2$ value was taken into account while evaluating the models. The $R^2$ value was calculated as 0.995 in the Langmuir isotherm model, 0.826 in the Freundlich isotherm, and 0.915 in the Temkin isotherm. As can be seen, the linearized version of the Langmuir isotherm model is very close to the experimental data. Therefore, it can be said that there is no interaction between the adsorbed molecules in general and the adsorption takes place in a single layer. In addition, the RL value, which is called the distribution constant, was calculated from the formula $RL = 1/(1 + aL.C_0)$, and it was examined whether the adsorption was favorable or not. Here, $a_L$ is the Langmuir constant (L/mg), and $C_0$ is the initial concentration of OTC. It is assumed that if the $R_L$ value is 0, it is irreversible; if it is between 0 and 1, it is favorable; if it is equal to 1, it is linear; if it is greater than 1, the isotherm is negative (Al-Ghouti & Da'ana, 2020; Weber & Chakravorti, 1974). In our study, the $R_L$ value was found to be 0.029, which is a favorable type of isotherm.

In addition, the maximum OTC concentration per unit adsorbent was calculated as 104.22 mg/g. It can be stated that the OTC at working pH is in cationic ($OTC^+$) and uncharged ($OTC^0$) form, interacting with the functional groups on the surface of the LPAC and adsorbed on the LPAC by replacing the hydroxyl groups in the LPAC in the adsorption process (Kan et al., 2017).

General assessment on removal efficiencies

In the literature, the extraction of AC from various wastes and the removal of some pollutants are examined and presented in Table 5. While the surface area of AC produced from LP at 500 °C in the presence of nitrogen gas was found to be 1158 $m^2$/g, Pb and malachite green dye removal were made with this AC at room temperature, and removal efficiencies
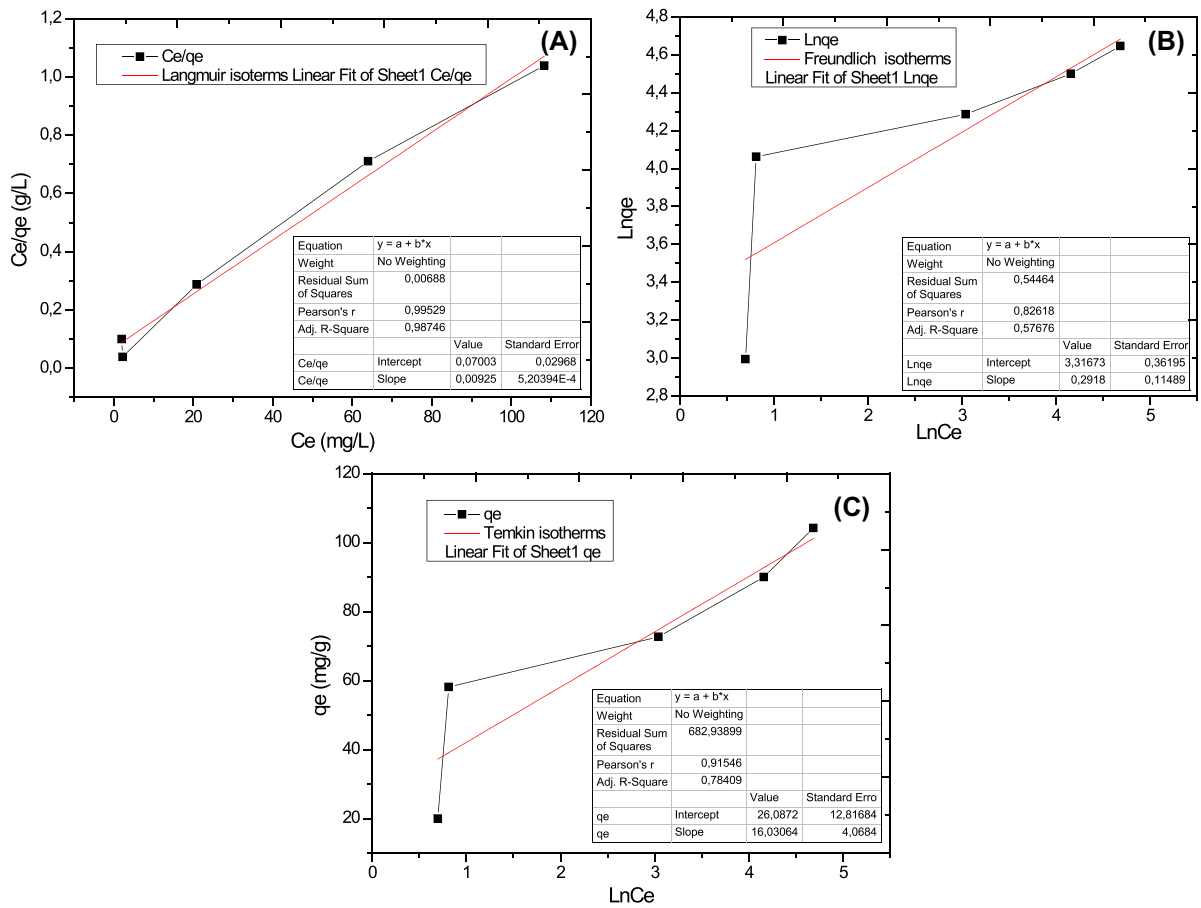
**Fig. 8** Adsorption isotherms for the removal of OTC, black line: (**A**) Langmuir isotherms, (**B**) Freundlich isotherms, (**C**) Temkin isotherms. The black dots represent the experimental run results, and the red line represents the linearized isotherms

of 90.91 mg/g in Pb and 66.67 mg/g in dye were obtained from the obtained AC (Mohammadi et al., 2014). Reactive blue 49 dye was removed with AC

**Table 4** Adsorption isotherm modeling for OTC removal

| İsotherm model | Constants and error functions | Value |
|---|---|---|
| Langmuir | $q_{max}$ (mg/g) | 104.22 |
| | $K_L$ (L/mg) | 14.29 |
| | $R_L$ (L/mg) | 0.029 |
| | $R^2$ | 0.995 |
| Freundlich | $1/n$ | 13.85 |
| | $K_F$ ($mg^{1-(1/n)} L^{1/n}/g$) | 2073.48 |
| | $R^2$ | 0.87 |
| Temkin | $A_T$ (L/mg) | 16.03 |
| | $b_T$ (g.J/(mg.mol)) | 26.09 |
| | $R^2$ | 0.92 |

obtained from LP at 300 °C, and the approximate removal efficiency was calculated as 50 mg/g (Taifi et al., 2022). On the other hand, the drug residue (OTC) was removed with AC obtained from waste tea pulp, and OTC removal efficiency was obtained at a maximum rate of 273.3 mg/g in the study (Kan et al., 2017), and a maximum of 230.84 mg/g OTC removal was achieved with AC obtained from forest residues and wood processing process wastes (Aghababaei et al., 2017). In our study, LP was converted into LPAC at 800 °C, and OTC removal was obtained at the rate of 104.22 mg/g.

*Statistical analysis*

To statistically evaluate (Minitab statistical software 19) which adsorbent amount change significantly influence the studied responses, an analysis

**Table 5** Comparison of the obtained values with the literature

| | This study | (Ramutshatsha-Makhwedzha et al., 2022) | (Bhatnagar et al., 2009) | (Mohammadi et al., 2014) | (Taifi et al., 2022) | (Sun et al., 2012) | (Kan et al., 2017) | (Berger et al., 2019) | (Aghababaei et al., 2017) |
|---|---|---|---|---|---|---|---|---|---|
| AC origin | Lemon Pulp | Orange and lemon peels | Lemon peel | Lemon peel | Lemon peel | Cotton linter fibers | Waste tea | Haas Avocados | F.R[1] and W.P.R[2] |
| AC preparation chemical | KOH | $H_3PO_4$ | - | $H_3PO_4$ | $H_3PO_4$ | NaOH | $H_3PO_4$ | KOH | $H_3PO_4$, $H_2SO_4$, NaOH, KOH |
| Gas type used in the preparation of AC | Ar | - | Air | Nitrogen | - | - | Nitrogen/air | Nitrogen | Nitrogen |
| AC preparation temperature (°C) | 800 | 600 | 500 | 500 | 300 | 700–850 | 450 | 600–900 | 400 and 600 |
| BET-surface area ($S_{BET}$: $m^2/g$) | 1333.1 | 1682.9 | - | 1158 | - | 2143 | 880 | 1156 | max.421.84 |
| BET-pore volume ($cm^3/g$) | 0.394 | 0.269 | - | - | - | - | 0.680 | - | - |
| Experiment volume (mL) | 50 | 50 | 50 | 20 | 100 | 100 | 50 | 40 | 10 |
| Mixing speed (rpm) | 60–240 | - | - | 240 | 300 | 125 | 150 | - | 220 |
| Experiment time | 75 min | 5–180 min | 60 min | 35 min | - | - | 35 h | - | 72 h |
| pH's studied | 2.0–8.0 | 2.0–10.0 | 5.5–6.5 | 7.0 | | 2.0–12.0 | - | 4.0–8.66 | 2.0–10.0 |
| Experiment temperature $^0$C | 25 | - | 25–45 | 25 | 15, 25, 35 | - | 20, 30, 40 | - | 20–40 |
| Pollutant type removed | OTC | Methyl orange and methylene | Methyl orange | Malachite green | Reactive blue 49 | OTC | OTC | OTC | OTC |
| Initial concentrations (mg/L) | 10–150 | 5–200 | - | 50–500 | 50–500 | 308.2–530.3 | 200−700 | 5–80 | 50 |
| Adsorption capacity of AC (mg/g) | 104.222 | Max 38.0 | 50.3 | 66.67 | ~50 | 144.6- 389.3 | max 273.7 | 140 | 263.78[2] |
| Adsorbent amount (g) | 0.005–0.08 | 0.010–0.8 | 0.1 | 0.2 | 0.05 | 0.06 | 0.05 | - | |

[1]Forest residues: 1 M $H_3PO_4$/600 °C

[2]Wood-processing residues: 5 M $H_3PO_4$/600 °C

- No information

**Table 6** Analyzes of variance (ANOVA) obtained for evaluated response at 95% confidence level
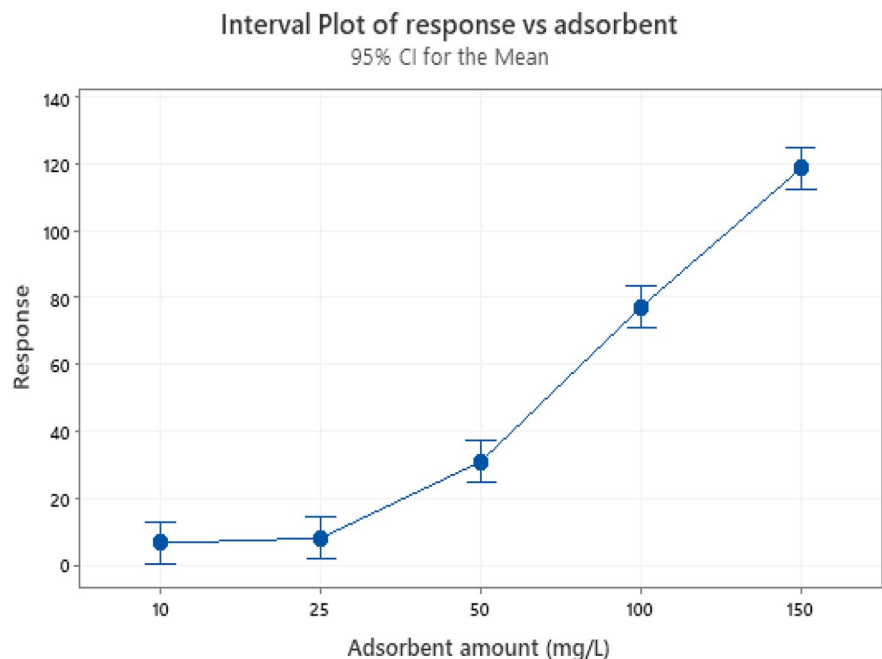
| Responses | Sum of square | df | Mean of square | F-test | p value |
|---|---|---|---|---|---|
| Adsorbent (mg/L) | $1.32 \times 10^2$ | 1 | $1.32 \times 10^2$ | 1.45 | 0.02 |

of variance was performed, and the obtained result are described in Table 6. The *p* value obtained at 95% confidence level indicates that of adsorbent amount was a factor with influence on the considered responses ($p > 0.05$ for responses). $R^2$ and $R^2$(adj) values in the model summary were obtained as 95.64% and 95.44%, respectively. The response value depending on the change in the amount of adsorbent obtained as a result of the analysis of variance is given in Fig. 9. Accordingly, as the amount of adsorbent increases, the response value also increases. Regression equation was as follow:

**Response** $= -4.81 + 0.697A + 0.000899\,A^2$ (A : adsorbent amount (mg/L)

## Conclusions

In this study, highly porous and mesoporous LPAC was produced from Lemon Pulp, and its structural characteristics and properties were analyzed, and OTC adsorption tests were performed and tried to be explained with mathematical models. According to the results obtained, LPAC, which is produced even at low temperatures such as 800 °C, has good removal efficiency even at much higher concentrations than the OTC concentrations that are likely to be encountered in aquatic environments. This study has demonstrated the usability of activated carbon obtained from LP in the removal of drug residues in existing and prospective treatment plants. Investigation of the reuse of used LPAC in future studies by regeneration (chemical treatment, extraction with supercritical flow, thermal degradation, etc.) is an issue worth investigating in terms of green sustainability.

**Fig. 9** Interval plot of response vs adsorbent

**Data availability** The datasets generated during and/or analyzed during the current study are available from the corresponding author on reasonable request.

**Declarations**

**Ethical approval** All authors have read, understood, and have complied as applicable with the statement on "Ethical responsibilities of Authors" as found in the Instructions for Authors and are aware that with minor exceptions, no changes can be made to authorship once the paper is submitted.

**Consent to participate** All authors have given consent to their contribution.

**Consent for publication** All authors have agreed with the content and all have given explicit consent to publish.

**Competing interests** The authors declare no competing interests.

# References

Abdollahzadeh, H., Fazlzadeh, M., Afshin, S., Arfaeinia, H., Feizizadeh, A., Poureshgh, Y., & Rashtbari, Y. (2020). Efficiency of activated carbon prepared from scrap tires magnetized by Fe3O4 nanoparticles: Characterisation and its application for removal of reactive blue19 from aquatic solutions. *102*(8), 1911–1925. https://doi.org/10.1080/03067319.2020.1745199

Adams, C., Asce, M., Wang, Y., Loftin, K., & Meyer, M. (2002). Removal of antibiotics from surface and distilled water in conventional water treatment processes related papers. *Journal of Environmental Engineering, 128*(3), 253. https://doi.org/10.1061/(ASCE)0733-9372(2002)128:3(253)

Adeleye, A. T., Akande, A. A., Odoh, C. K., Philip, M., Fidelis, T. T., Amos, P. I., & Banjoko, O. O. (2021). Efficient synthesis of bio-based activated carbon (AC) for catalytic systems: A green and sustainable approach.

*Journal of Industrial and Engineering Chemistry, 96*, 59–75. https://doi.org/10.1016/J.JIEC.2021.01.044

Afshin, S., Rashtbari, Y., Ramavandi, B., Fazlzadeh, M., Vosoughi, M., Mokhtari, S. A., et al. (2020). Magnetic nanocomposite of filamentous algae activated carbon for efficient elimination of cephalexin from aqueous media. *Korean Journal of Chemical Engineering, 37*(1), 80–92. https://doi.org/10.1007/S11814-019-0424-6/METRICS

Aghababaei, A., Ncibi, M. C., & Sillanpää, M. (2017). Optimized removal of oxytetracycline and cadmium from contaminated waters using chemically-activated and pyrolyzed biochars from forest and wood-processing residues. *Bioresource Technology, 239*, 28–36. https://doi.org/10.1016/J.BIORTECH.2017.04.119

Ahmadfazeli, A., Poureshgh, Y., Rashtbari, Y., Akbari, H., Pourali, P., & Adibzadeh, A. (2021). Removal of metronidazole antibiotic from aqueous solution by ammonia-modified activated carbon: Adsorption isotherm and kinetic study. *Journal of Water, Sanitation and Hygiene for Development, 11*(6), 1083–1096. https://doi.org/10.2166/WASHDEV.2021.117

Al-Gheethi, A. A. S., Lalung, J., Noman, E. A., Bala, J. D., & Norli, I. (2015). Removal of heavy metals and antibiotics from treated sewage effluent by bacteria. *Clean Technologies and Environmental Policy, 17*(8), 2101–2123. https://doi.org/10.1007/S10098-015-0968-Z

Al-Ghouti, M. A., & Da'ana, D. A. (2020). Guidelines for the use and interpretation of adsorption isotherm models: A review. *Journal of Hazardous Materials, 393*, 122383. https://doi.org/10.1016/J.JHAZMAT.2020.122383

Al-Qodah, Z., & Shawabkah, R. (2009). Production and characterization of granular activated carbon from activated sludge. *Brazilian Journal of Chemical Engineering, 26*(1), 127–136. https://doi.org/10.1590/S0104-66322009000100012

Avisar, D., Lester, Y., & Ronen, D. (2009). Sulfamethoxazole contamination of a deep phreatic aquifer. *Science of the Total Environment, 407*(14), 4278–4282. https://doi.org/10.1016/J.SCITOTENV.2009.03.032

Ayawei, N., Ebelegi, A. N., & Wankasi, D. (2017). Modelling and interpretation of adsorption isotherms. *Journal of Chemistry*, *2017*. https://doi.org/10.1155/2017/3039817

Balzer, F., Zöhlke, S., & Hannappel, S. (2016). Antibiotics in groundwater under locations with high livestock density in Germany. *Water Supply, 16*(5), 1361–1369. https://doi.org/10.2166/WS.2016.050

Beltrame, K. K., Cazetta, A. L., de Souza, P. S. C., Spessato, L., Silva, T. L., & Almeida, V. C. (2018). Adsorption of caffeine on mesoporous activated carbon fibers prepared from pineapple plant leaves. *Ecotoxicology and Environmental Safety, 147*, 64–71. https://doi.org/10.1016/J.ECOENV.2017.08.034

Berger, M., Ford, J., & Goldfarb, J. L. (2019). Modeling aqueous contaminant removal due to combined hydrolysis and adsorption: Oxytetracycline in the presence of biomass-based activated carbons. *Separation Science and Technology (philadelphia), 54*(5), 705–721. https://doi.org/10.1080/01496395.2018.1520721/SUPPL_FILE/LSST_A_1520721_SM9779.DOCX

Bhatnagar, A., Kumar, E., Minocha, A. K., Jeon, B. H., Song, H., & Seo, Y. C. (2009). Removal of anionic dyes from

water using Citrus limonum (lemon) peel: Equilibrium studies and kinetic modeling. *44*(2), 316–334. https://doi.org/10.1080/01496390802437461

Braghiroli, F. L., Bouafif, H., Neculita, C. M., & Koubaa, A. (2018). Activated biochar as an effective sorbent for organic and inorganic contaminants in water. *Water, Air, and Soil Pollution, 229*(7), 1–22. https://doi.org/10.1007/S11270-018-3889-8/TABLES/1

Chen, X., & Yao, M. (2015). Modeling of experimental adsorption isotherm data. *Information, 6*(1), 14–22. https://doi.org/10.3390/INFO6010014

Chen, G., Wu, G., Li, N., Lu, X., Zhao, J., He, M., et al. (2021). Landfill leachate treatment by persulphate related advanced oxidation technologies. *Journal of Hazardous Materials, 418*, 126355. https://doi.org/10.1016/J.JHAZMAT.2021.126355

Daghrir, R., & Drogui, P. (2013). Tetracycline antibiotics in the environment: A review. *Environmental Chemistry Letters, 11*(3), 209–227. https://doi.org/10.1007/S10311-013-0404-8

Farahani, M., Abdullah, S. R. S., Hosseini, S., Shojaeipour, S., & Kashisaz, M. (2011). Adsorption-based cationic dyes using the carbon active sugarcane bagasse. *Procedia Environmental Sciences*, *10*(PART A), 203–208. https://doi.org/10.1016/J.PROENV.2011.09.035

Foo, K. Y., & Hameed, B. H. (2012). Coconut husk derived activated carbon via microwave induced activation: Effects of activation agents, preparation parameters and adsorption performance. *Chemical Engineering Journal, 184*, 57–65. https://doi.org/10.1016/J.CEJ.2011.12.084

Freundlich, H. M. F. (1906). Over the adsorption in solution. *Journal of Physical Chemistry, 57*(385471), 1100–1107.

Gaballah, M. S., Guo, J., Sun, H., Aboagye, D., Sobhi, M., Muhmood, A., & Dong, R. (2021). A review targeting veterinary antibiotics removal from livestock manure management systems and future outlook. *Bioresource Technology, 333*, 125069. https://doi.org/10.1016/J.BIORTECH.2021.125069

Hashem, A., Aniagor, C. O., Nasr, M. F., & Abou-Okeil, A. (2021). Efficacy of treated sodium alginate and activated carbon fibre for Pb(II) adsorption. *International Journal of Biological Macromolecules, 176*, 201–216. https://doi.org/10.1016/J.IJBIOMAC.2021.02.067

Ho, Y. S., Wase', D., & Forster, C. F. (1996). Removal of lead ions from aqueous solution using sphagnum moss peat as adsorbent. *Water SA, 22*(3), 214–219.

Huang, F., An, Z., Moran, M. J., & Liu, F. (2020). Recognition of typical antibiotic residues in environmental media related to groundwater in China (2009–2019). *Journal of Hazardous Materials, 399*, 122813. https://doi.org/10.1016/J.JHAZMAT.2020.122813

Huang, A., Yan, M., Lin, J., Xu, L., Gong, H., & Gong, H. (2021). A review of processes for removing antibiotics from breeding wastewater. *International Journal of Environmental Research and Public Health, 18*(9), 4909. https://doi.org/10.3390/IJERPH18094909

Hui, T., & Zaini, M. (2015). Potassium hydroxide activation of activated carbon: A commentary. *Carbon Letters, 16*(4), 275–280.

Joseph, C. G., Zain, H. F. M., & Dek, S. F. (2006). Treatment of landfill leachate in Kayu Madang, Sabah: Textural and physical characterızatıon (part 1). *Malaysia Journal of Analytical Sciences, 10*(1), 1–6.

Kan, Y., Yue, Q., Li, D., Wu, Y., & Gao, B. (2017). Preparation and characterization of activated carbons from waste tea by H3PO4 activation in different atmospheres for oxytetracycline removal. *Journal of the Taiwan Institute of Chemical Engineers, 71*, 494–500. https://doi.org/10.1016/J.JTICE.2016.12.012

Karthikeyan, K. G., & Meyer, M. T. (2006). Occurrence of antibiotics in wastewater treatment facilities in Wisconsin, USA. *Science of the Total Environment, 361*(1–3), 196–207. https://doi.org/10.1016/J.SCITOTENV.2005.06.030

Klein, E. Y., Van Boeckel, T. P., Martinez, E. M., Pant, S., Gandra, S., Levin, S. A., et al. (2018). Global increase and geographic convergence in antibiotic consumption between 2000 and 2015. *Proceedings of the National Academy of Sciences of the United States of America, 115*(15), E3463–E3470. https://doi.org/10.1073/PNAS.1717295115

Kumar Jha, M., Joshi, S., Sharma, R. K., Kim, A. A., Pant, B., Park, M., & Pant, H. R. (2021). Surface modified activated carbons: Sustainable bio-based materials for environmental remediation. https://doi.org/10.3390/nano11113140

Kümmerer, K., Al-Ahmad, A., & Mersch-Sundermann, V. (2000). Biodegradability of some antibiotics, elimination of the genotoxicity and affection of wastewater bacteria in a simple test. *Chemosphere, 40*(7), 701–710. https://doi.org/10.1016/S0045-6535(99)00439-7

Lach, J., Ociepa-Kubicka, A., & Mrowiec, M. (2021). Oxytetracycline adsorption from aqueous solutions on commercial and high-temperature modified activated carbons. *Energies, 14*(12), 3481. https://doi.org/10.3390/EN14123481

Langbehn, R. K., Michels, C., & Soares, H. M. (2021). Antibiotics in wastewater: From its occurrence to the biological removal by environmentally conscious technologies. *Environmental Pollution, 275*, 116603. https://doi.org/10.1016/J.ENVPOL.2021.116603

Langmuir, I. (1916). The constitution and fundamental properties of solids and liquids. Part I. Solids. *Journal of the American Chemical Society, 38*(11), 2221–2295. https://doi.org/10.1021/JA02268A002/ASSET/JA02268A002.FP.PNG_V03

Li, D., Shao, H., Huo, Z., Xie, N., Gu, J., & Xu, G. (2021). Typical antibiotics in the receiving rivers of direct-discharge sources of sewage across Shanghai: Occurrence and source analysis. *RSC Advances, 11*(35), 21579–21587. https://doi.org/10.1039/D1RA02510D

Lien, L. T. Q., Hoa, N. Q., Chuc, N. T. K., Thoa, N. T. M., Phuc, H. D., Diwan, V., et al. (2016). Antibiotics in wastewater of a rural and an urban hospital before and after wastewater treatment, and the relationship with antibiotic use—A one year study from Vietnam. *International Journal of Environmental Research and Public Health, 13*(6), 588. https://doi.org/10.3390/IJERPH13060588

Liu, X., Steele, J. C., & Meng, X. Z. (2017). Usage, residue, and human health risk of antibiotics in Chinese aquaculture: A review. *Environmental Pollution, 223*, 161–169. https://doi.org/10.1016/J.ENVPOL.2017.01.003

Mamaní, A., Ramírez, N., Deiana, C., Giménez, M., & Sardella, F. (2019). Highly microporous sorbents from

lignocellulosic biomass: Different activation routes and their application to dyes adsorption. *Journal of Environmental Chemical Engineering, 7*(5), 103148.

Masinga, T., Moyo, M., & Pakade, V. E. (2022). Removal of hexavalent chromium by polyethyleneimine impregnated activated carbon: Intra-particle diffusion, kinetics and isotherms. *Journal of Materials Research and Technology, 18*, 1333–1344. https://doi.org/10.1016/J.JMRT.2022.03.062

Mohammadi, S. Z., Karimi, M. A., Yazdy, S. N., Shamspur, T., & Hamidian, H. (2014). Removal of Pb(II) ions and malachite green dye from wastewater by activated carbon produced from lemon peel. *Química Nova, 37*(5), 804–809. https://doi.org/10.5935/0100-4042.20140129

MozaffariMajd, M., Kordzadeh-Kermani, V., Ghalandari, V., Askari, A., & Sillanpää, M. (2022). Adsorption isotherm models: A comprehensive and systematic review (2010–2020). *Science of The Total Environment, 812*, 151334. https://doi.org/10.1016/J.SCITOTENV.2021.151334

Muhammad, J., Khan, S., Su, J. Q., Hesham, A. E. L., Ditta, A., Nawab, J., & Ali, A. (2020). Antibiotics in poultry manure and their associated health issues: A systematic review. *Journal of Soils and Sediments, 20*(1), 486–497. https://doi.org/10.1007/S11368-019-02360-0/FIGURES/5

Naeem, S., Baheti, V., Tunakova, V., Militky, J., Karthik, D., & Tomkova, B. (2017). Development of porous and electrically conductive activated carbon web for effective EMI shielding applications. *Carbon, 111*, 439–447. https://doi.org/10.1016/J.CARBON.2016.10.026

Nayeri, D., Mousavi, S. A., & Mehrabi, A. (2019). Oxytetracycline removal from aqueous solutions using activated carbon prepared from corn stalks. *Journal of Applied Research in Water and Wastewater, 6*(1), 67–72. https://doi.org/10.22126/ARWW.2019.1136

Okon Eddy, N., Garg, R., Garg, · Rishav, Augustine, ·, Aikoye, O., Benedict, ·, & Ita, I. (2022). Waste to resource recovery: Mesoporous adsorbent from orange peel for the removal of trypan blue dye from aqueous solution. *Biomass Conversion and Biorefinery*, *1*, 3.https://doi.org/10.1007/s13399-022-02571-5

Ötker, H. M., & Akmehmet-Balcioğlu, I. (2005). Adsorption and degradation of enrofloxacin, a veterinary antibiotic on natural zeolite. *Journal of Hazardous Materials, 122*(3), 251–258. https://doi.org/10.1016/J.JHAZMAT.2005.03.005

Peyghami, A., Moharrami, A., Rashtbari, Y., Afshin, S., Vosuoghi, M., & Dargahi, A. (2021). Evaluation of the efficiency of magnetized clinoptilolite zeolite with Fe3O4 nanoparticles on the removal of basic violet 16 (BV16) dye from aqueous solutions. *44*(2), 278–287. https://doi.org/10.1080/01932691.2021.1947847

Qiu, H., Lv, L., Pan, B. C., Zhang, Q. J., Zhang, W. M., & Zhang, Q. X. (2009). Critical review in adsorption kinetic models. *Journal of Zhejiang University-SCIENCE A, 10*(5), 716–724. https://doi.org/10.1631/JZUS.A0820524

Rajahmundry, G. K., Garlapati, C., Kumar, P. S., Alwi, R. S., & Vo, D. V. N. (2021). Statistical analysis of adsorption isotherm models and its appropriate selection. *Chemosphere, 276*, 130176. https://doi.org/10.1016/J.CHEMOSPHERE.2021.130176

Ramutshatsha-Makhwedzha, D., Mavhungu, A., Moropeng, M. L., & Mbaya, R. (2022). Activated carbon derived from waste orange and lemon peels for the adsorption of

methyl orange and methylene blue dyes from wastewater. *Heliyon*, *8*(8). https://doi.org/10.1016/J.HELIYON.2022.E09930

Rashtbari, Y., Américo-Pinheiro, J. H. P., Bahrami, S., Fazlzadeh, M., Arfaeinia, H., & Poureshgh, Y. (2020). Efficiency of zeolite coated with zero-valent iron nanoparticles for removal of humic acid from aqueous solutions. *Water, Air, and Soil Pollution, 231*(10), 1–15. https://doi.org/10.1007/S11270-020-04872-9/FIGURES/7

Rashtbari, Y., Afshin, S., Hamzezadeh, A., Gholizadeh, A., Ansari, F. J., Poureshgh, Y., & Fazlzadeh, M. (2022). Green synthesis of zinc oxide nanoparticles loaded on activated carbon prepared from walnut peel extract for the removal of Eosin Y and Erythrosine B dyes from aqueous solution: Experimental approaches, kinetics models, and thermodynamic studies. *Environmental Science and Pollution Research, 29*(4), 5194–5206. https://doi.org/10.1007/S11356-021-16006-7/FIGURES/5

Russell, J. N., & Yost, C. K. (2021). Alternative, environmentally conscious approaches for removing antibiotics from wastewater treatment systems. *Chemosphere, 263*, 128177. https://doi.org/10.1016/J.CHEMOSPHERE.2020.128177

Shokoohi, R., Samadi, M. T., Amani, M., & Poureshgh, Y. (2018a). Modeling and optimization of removal of cefalexin from aquatic solutions by enzymatic oxidation using experimental design. *Brazilian Journal of Chemical Engineering, 35*(3), 943–956. https://doi.org/10.1590/0104-6632.20180353S20170383

Shokoohi, R., Samadi, M. T., Amani, M., & Poureshgh, Y. (2018b). Optimizing laccase-mediated amoxicillin removal by the use of box–behnken design in an aqueous solution. *Desalination and Water Treatment, 119*, 53–63. https://doi.org/10.5004/DWT.2018.21922

Singh, S. A., & Shukla, ● S R. (n.d.). Adsorptive removal of cobalt ions on raw and alkali-treated lemon peels. *International Journal of Environmental Science and Technology*. https://doi.org/10.1007/s13762-015-0801-6

Sta Ana, K. M., Madriaga, J., & Espino, M. P. (2021). β-Lactam antibiotics and antibiotic resistance in Asian lakes and rivers: An overview of contamination, sources and detection methods. *Environmental Pollution, 275*, 116624. https://doi.org/10.1016/J.ENVPOL.2021.116624

Sun, Y., Yue, Q., Gao, B., Li, Q., Huang, L., Yao, F., & Xu, X. (2012). Preparation of activated carbon derived from cotton linter fibers by fused NaOH activation and its application for oxytetracycline (OTC) adsorption. *Journal of Colloid and Interface Science, 368*(1), 521–527. https://doi.org/10.1016/J.JCIS.2011.10.067

Sun, Y., Yue, Q., Gao, B., Wang, Y., Gao, Y., & Li, Q. (2013). Preparation of highly developed mesoporous activated carbon by H4P2O7 activation and its adsorption behavior for oxytetracycline. *Powder Technology, 249*, 54–62. https://doi.org/10.1016/J.POWTEC.2013.07.029

Taifi, A., Alkadir, O. K. A., Aljeboree, A. M., Bayaa, A. L. Al, Alkaim, A. F., & Abed, S. A. (2022). Environmental removal of reactive blue 49 dye from aqueous solution by (lemon peels as activated carbon): A model of low cost agricultural waste. *IOP Conference Series: Earth and Environmental Science*, *1029*(1), 012010.https://doi.org/10.1088/1755-1315/1029/1/012010

Temkin, M. I. (1940). Kinetics of ammonia synthesis on promoted iron catalysts. *Acta Physiochim, 12*, 327–356.

Thirumavalavan, M., Lai, Y. L., & Lee, J. F. (2011). Fourier transform infrared spectroscopic analysis of fruit peels before and after the adsorption of heavy metal ions from aqueous solution. *Journal of Chemical and Engineering Data, 56*(5), 2249–2255. https://doi.org/10.1021/JE101262W

Tiseo, K., Huber, L., Gilbert, M., Robinson, T. P., & Van Boeckel, T. P. (2020). Global trends in antimicrobial use in food animals from 2017 to 2030. *Antibiotics, 9*(12), 918. https://doi.org/10.3390/ANTIBIOTICS9120918

Wang, J., & Guo, X. (2020). Adsorption isotherm models: Classification, physical meaning, application and solving method. *Chemosphere, 258*, 127279. https://doi.org/10.1016/J.CHEMOSPHERE.2020.127279

Wang, J., & Guo, X. (2020). Adsorption kinetic models: Physical meanings, applications, and solving methods. *Journal of Hazardous Materials, 390*, 122156. https://doi.org/10.1016/J.JHAZMAT.2020.122156

Wang, J., & Zhuan, R. (2020). Degradation of antibiotics by advanced oxidation processes: An overview. *Science of The Total Environment, 701*, 135023. https://doi.org/10.1016/J.SCITOTENV.2019.135023

Watts, C. D., Crathorne, B., Fielding, M., & Steel, C. P. (1984). Identification of non-volatile organics in water using field desorption mass spectrometry and high performance liquid chromatography. *Analysis of Organic Micropollutants in Water*, 120–131. https://doi.org/10.1007/978-94-009-6345-0_13

Weber, T. W., & Chakravorti, R. K. (1974). Pore and solid diffusion models for fixed-bed adsorbers. *AIChE Journal, 20*(2), 228–238. https://doi.org/10.1002/AIC.690200204

Westerhoff, P., Yoon, Y., Snyder, S., & Wert, E. (2005). Fate of endocrine-disruptor, pharmaceutical, and personal care product chemicals during simulated drinking water treatment processes. *Environmental Science and Technology, 39*(17), 6649–6663. https://doi.org/10.1021/ES0484799/SUPPL_FILE/ES0484799SI20050607_060544.PDF

Yang, Y., Song, W., Lin, H., Wang, W., Du, L., & Xing, W. (2018). Antibiotics and antibiotic resistance genes in global lakes: A review and meta-analysis. *Environment International, 116*, 60–73. https://doi.org/10.1016/J.ENVINT.2018.04.011

Zainab, S. M., Junaid, M., Xu, N., & Malik, R. N. (2020). Antibiotics and antibiotic resistant genes (ARGs) in groundwater: A global review on dissemination, sources, interactions, environmental and human health risks. *Water Research, 187*, 116455. https://doi.org/10.1016/J.WATRES.2020.116455

Zdravkov, B. D., Čermák, J. J., Šefara, M., & Janků, J. (2007). Pore classification in the characterization of porous materials: A perspective. *Central European Journal of Chemistry, 5*(2), 385–395. https://doi.org/10.2478/S11532-007-0017-9/MACHINEREADABLECITATION/RIS